Electron transfer modifies chemical properties of C-70 fullerene surface: An ab initio molecular dynamics study of C70O3 molozonides doped with light atoms

Bil, Andrzej ; Hutter, Juerg ; Morrison, Carole A

Abstract: Light metal atoms such as Li, K (electronic state S-2(1/2)) or Ca (S-1(0)) encapsulated in a C-70 cage considerably modifies the chemical properties of the fullerene surface due to metal-to-cage electron transfer. H-doped and anion ozonide systems were also considered to validate the electron transfer hypothesis. The relative stabilities of the eight isomers of the C70O3 molozonide series at room temperature depend on the identity of the endohedral guest, as was the preferred channel for thermal decomposition. No electron transfer was observed for the complex N@C-70 where the fullerene acts as an inert container for the S-4(3/2) radical. (C) 2014 Elsevier B.V. All rights reserved.

DOI: https://doi.org/10.1016/j.cplett.2014.05.025

Electron transfer modifies chemical properties of C_{70} fullerene surface. An ab Initio molecular dynamics study of $C_{70}O_3$ molozonides doped with light atoms.

Andrzej Bil,*[,a,b], Jürg Hutter,[a] Carole A. Morrison[c]

[a] Institute of Physical Chemistry, University of Zürich, Winterthurerstrasse 190, CH-8057 Zürich, Switzerland

[b]Faculty of Chemistry, University of Wrocław F. Joliot Curie 14, 50-383 Wrocław Poland

[c] School of Chemistry and EaSTCHEM Research School, The University of Edinburgh, King's Buildings, West Mains Road, Edinburgh, EH9 3JJ, UK

**** abil@elrond.chem.uni.wroc.pl***

Abstract

Light metal atoms such as Li, K (electronic state $^2S_{1/2}$) or Ca ($^1S_0$) encapsulated in a C_{70} cage considerably modifies the chemical properties of the fullerene surface due to metal-to-cage electron transfer. H-doped and anion ozonide systems were also considered to validate the electron transfer hypothesis. The relative stabilities of the eight isomers of the $C_{70}O_3$ molozoide series at room temperature depend on the identity of the endohedral guest, as was the preferred channel for thermal decomposition. No electron transfer was observed for the complex N@C_{70} where the fullerene acts as an inert container for the $^4S_{3/2}$ radical.

Keywords: electron transfer, endohedral guest, reaction mechanism, DFT

Introduction

Advanced synthetic methods and new separation techniques have contributed to the rapid development observed in endohedral metallofullerene (EMF) chemistry.[1] Data obtained from the growing number of known EMFs indicate that the chemical properties of these structures are different from those of the parent empty fullerene, which is believed to result from electron transfer from the metal to the cage.[2] The list of structurally characterized monometallofullerenes is dominated by the higher members (C_n, n > 70) doped with heavy metal atoms (such as lanthanides or group 3 metals), and many interesting results have been obtained in the chemistry of such complexes.[2-5] However, much less is known about the properties of C_{60} and C_{70} doped with lighter metal atoms, despite the fact that lithium complexes with these fullerenes were amongst the first EMFs to be obtained using ion implantation techniques.[6,7] This method was also used to prepare endohedral complexes of light fullerenes encapsulating a single N atom,[8] creating materials with potential application in quantum computing.[9]

C_{70} is more challenging for computational investigation than C_{60} as it is larger and has eight non-equivalent bonding environments, compared to just two for C_{60}. On the other hand, derivatives of C_{70}, such as monoozonides,[10] serve as a rich model system for theoretical study into how endohedral modifications influence the properties of the carbon cage.[11,12] Layers of equivalent carbon atoms in C_{70} are typically labelled from ‘a’ to ‘e’ , which also serves as a convenient way to label equivalent C-C bonds, and to categorise the 37 rings into one of five types (Figure 1). Of the eight possible types of C-C bond, C_a-C_b and C_c-C_c exhibit features typical of double bonds, while the others are considered to be more like single bonds, with various contributions from the neighbouring π-electron density.[10,13] Not surprisingly, a,b-$C_{70}O_3$ and c,c-$C_{70}O_3$, the only two isomers known experimentally, are also the most thermodynamically stable isomers, according to recent computational results.[14]

Molecular dynamics simulations indicate that apart from e,e-$C_{70}O_3$, all other ozonide isomers remain stable at room temperature. For the isomer where the O_3 unit bridges the C-C bond in the equatorial belt, we have previously reported a spontaneous ring opening reaction during the course of an *ab initio* MD run; the process (1) → (2) is depicted schematically in Figure 2.[14] We also investigated a series of isomers doped with noble gas atoms[11] and light molecules.[12] These calculations indicated that the endohedral guest does not appear to influence the

dynamic behavior of the isomer series, which means that, as for the empty ozonides, the spontaneous ring opening reaction was observed only for the isomer X@e,e-$C_{70}O_3$. We have also studied the influence of the guest on the relative stability of the isomer series, comparing the enthalpies of the ozonides calculated as a value averaged over an MD trajectory at 298K. We found that the calculated stabilities of the isomers depend only marginally on the identity of the guest. In the case of where ozonides are doped with a noble gas atom, the largest influence was observed for the complexes containing Xe and Rn atoms where the observed change in relative enthalpies was up to 3.5 kcal mol^{-1}. In the case of the lightest molecular guests, the relative isomer stabilities changed by some ± 1.5 kcal mol^{-1}, depending on the identity of the encapsulated molecule. A larger effect, up to 3.6 kcal mol^{-1}, was observed for the set of ozonides doped with two hydrogen molecules.

In this paper we now turn to investigate the influence of an endohedral guest, specifically Li and K (all $^2S_{1/2}$ electronic state), N ($^4S_{3/2}$) and Ca ($^1S_0$), on the surface chemical properties of C_{70} . As with our previous papers, we have chosen the ozone ring opening reaction in X@$C_{70}O_3$ as a model chemical reaction to study the influence of the guest on the reaction mechanism. We also study how the guest modifies the relative stabilities of the ozonide isomer series. In order to be able to discuss the results obtained in the context of guest-to-cage electron transfer we have also calculated structures doped with a single H atom, as well as $C_{70}O_3^-$ anions. Sharing the same $^2S_{1/2}$ electronic state these structures serve as computational models for the limiting cases where the unpaired electron resides either entirely on the guest atom (H@C_{70} and H@$C_{70}O_3$) or on the cage ($C_{70}O_3^-$). We start this account with a study of the dynamical behavior of the atomic guest inside the parent C_{70} fullerene cage.

Methods

All electronic structure calculation were performed using a Density Functional Theory based methodology. Open shell molecules are treated with the unrestricted spin-polarized approach. approach. Structure optimizations and molecular dynamics simulations were performed using the Becke-Lee-Yang-Parr exchange-correlation functional,[15,16] coupled to a Gaussian and plane-wave basis set,[17] as implemented in the QUICKSTEP program,[18] a part of the CP2K suite of software.[19] This functional has been successfully used to study structure and dynamics of C_{70} oxides and

ozonides[14] and their derivatives doped endohedrally with noble gas atoms[11] or light molecules.[12] Its hybrid counterpart, B3-LYP, proved to be useful in the analysis of the bonding situation and stability of isomers of $C_{70}O$ and $C_{70}O_3$.[13] The functional, whose correlation part, LYP, originates in an approximate correlation energy formula for helium as a reference system, as proposed by Cole and Salvetti,[20] is widely used to investigate chemical structures. For the B-LYP functional there are available well tested and computationally effective schemes to include dispersion contributions to the total energy,[21-24] which is particularly important for a proper description of intermolecular interactions. Long range dispersion interactions have been accounted for by using an approximate semi-empirical DFT-D3 correction scheme proposed by Grimme.[24] The importance of the dispersion correction in performing DFT-based simulations for the accurate modeling of chemical reactivity of fullerenes is well documented.[25] We used the Goedecker-Teter-Hutter norm-conservative pseudopotentials optimized for use against the BLYP functional, available as standard with the CP2K distribution.[26] Valence orbitals of C atoms were expanded using DZVP-GTH-BLYP and of the guest atoms using DZVP-MOLOPT-SR-GTH double-zeta quality basis sets.[27] The energy cutoff of 350 Ry was used to define an auxiliary basis set, together with cubic periodic boundary conditions to create a simulation cell of length 20 Å. For complexes containing a Li atom the energy cutoff was increased to 400 Ry. Following geometry optimization, Born-Oppenheimer MD simulations of ca. 20 ps duration were performed in the canonical ensemble, with a time step of 0.7 fs and a mean temperature of 298K regulated using a chain of Nose-Hoover thermostats. Atomic charges and spins were calculated according to the Mulliken population analysis.[28]

Results

First, some comments regarding the degree and nature of electron transfer between the encapsulated atom and the carbon cage. When the guest is a metal, electron transfer should occur. Indeed, the charges of the guest atoms averaged over the MD trajectories are 0.51±0.05e in $Li@C_{70}$, 0.53±0.05e in $Ca@C_{70}$ and 0.57±0.02e in $K@C_{70,}$ which indicates substantial electron density transfer from the atom to the fullerene molecule. The charges of all carbon atoms in $X@C_{70}$ are tabulated in Table S1 in Supplementary Materials. The actual charge of the metal

guest is dependent on the position of the guest inside the cage, therefore we observe some charge fluctuation along the MD trajectories (Figure S2, Supplementary Materials). The cages in K@C_{70} and Li@C_{70} are radicals, with the unpaired electron almost completely transferred to the cage from the guest atom (the α-β spin density localized on the guest atom and averaged over MD trajectory is 0.00±0.00e for both Li@C_{70} and K@C_{70} ; note Ca@C_{70} is a closed shell system). In N@C_{70} and H@C_{70} the amount of charge transfer from the cage to the guest is negligibly small (the averaged charge of the N atom is -0.05±0.03e and 0.05±0.01e for the H atom).. All spin density is concentrated on the guest atom for both of these systems.

In Figure 3 we present trajectories arced by the guest atoms N, K, Li and Ca inside C_{70} cages during the course of molecular dynamics simulations conducted at room temperature. From this we observe quite distinct behaviors. The N atom explores the space roughly between the two planes defined by the d-type carbon atoms (see Figure 1 for atom labelling). Similar dynamics were observed for noble gas atoms and some light molecules, e.g CH_4, NH_3, H_2O or HCl.[12] The heavier K atom, however, undergoes only small oscillations around its equilibrium (gravity center) position. Quite different behavior is observed for the Ca atom, which keeps to only one hemisphere and is slightly shifted towards the fullerene apex. Finally, the Li does not cross the d-planes and so avoids the apical part of the fullerene cage, but is instead attracted by the surface in the equatorial region of C_{70}.

To describe the behavior of the guest atom in C_{70} in a more quantitative way, we have calculated the distance of a guest atom from the center of each five or six-member carbon ring. When this procedure is repeated for each step of the MD run two key pieces of information are obtained. Firstly, we identify how often the atom sits over a given type of ring in the course of an MD run (Table S3, Supplementary Materials), and secondly we obtain the average distance between the atom and the preferred ring location (Table S4, Supplementary Materials).

In Li@C_{70}, the encapsulated atom tends to sit over the c-c-d-e-e-d (ca. 45% of the simulation time), the d-d-e-d-d-e (ca. 26%) and b-c-d-d-c rings (ca. 23%, see Figure 1 for atom labelling), with rather short average atom-to-ring distances of 1.92 Å, 1.95 Å and 1.99 Å, respectively, indicating that the Li atom is quite

strongly attracted to the fullerene surface. The preferred position of the Ca atom in the fullerene complex is in the proximity of the a-a-b-c-c-b ring-type, where the atom spends ca. 56% of the simulation time, 2.13 Å from the ring center on average. The K atom tends to oscillate around the fullerene center, keeping an average distance of 3.27 Å from the center of the c-c-d-e-e-d ring, over which the atom is present for ca. 66% of the MD trajectory.

In H@C_{70} the average distance between the H atom and the nearest ring is ca. 2.47 Å, while the most frequently 'visited' part of the fullerene is in the proximity of the a-a-b-c-c-b rings (ca. 61% of the MD trajectory). For N@C_{70} the endohedral atom tends to approach rings a-a-b-c-c-b (ca. 44%) and c-c-d-e-e-d (33%) most frequently, with average distances of 2.73 Å and 2.90 Å, respectively.

An alternative way to present the behavior of a guest atom inside C_{70} can be obtained by plotting the trajectory of the guest as a function of the simulation time. A convenient way to achieve this is to embed the Cartesian coordinate system into the fullerene cage and then describe the position of the guest in terms of spherical coordinates. The details of the procedure, as well as the dynamics of the N, K, Li and Ca atoms in X@C_{70} complexes are presented in Figures S3 – S7, Supplementary Materials.

The volume of the carbon atom cage, averaged over the MD trajectories, is influenced only marginally by the presence of the endohedral guest (Table S5, Supplementary Materials). The largest increase in the volume is observed for Ca@C_{70} and K@C_{70} (215.2 $Å^3$, comparing to 213.6 $Å^3$ for the empty fullerene[12]).

Turning the discussion now to the reactivity of the fullerene surface, molecular dynamics simulations performed for the ozonide series of isomers doped with guest atoms indicate that the guest can essentially influence the mechanism of the ozone ring opening reaction. For complexes containing encapsulated N or H atoms, the spontaneous ozone ring opening is observed only for the N/H@e,e-$C_{70}O_3$ isomer, and the process follows the mechanism (1)→(2) as shown in Figure 2. This reproduces the behavior observed in the course of MD runs for empty ozonides.[14] The reaction does not take place for Ca@e,e-$C_{70}O_3$, even though the simulation was extended to as long as 30ps. Interestingly, the ring opening reaction consistent with mechanism (1)→(2) was observed for Ca@d,d-$C_{70}O_3$ isomer, something which was not observed for the empty d,d-$C_{70}O_3$. We will return to this point later.

For ozonides doped with Li and K it seems that two competing processes for ozone ring decomposition in the e,e isomer are possible. In K@e,e-$C_{70}O_3$ the reaction follows the (1)→(2) mechanism, in common with the empty fullerene cage, and when the cage is doped with a noble gas or a light molecule. Li@e,e-$C_{70}O_3$ tends to follow the mechanism (1)→(3)→(5) (Figure 2), which is triggered by the dissociation of the C-O and O-O bonds, and leads to the release of an O_2 molecule. In the next step, the oxygen atom with an unsaturated valency in the $C_{70}O$ transient structure (Figure 2, structure 3) bridges the adjacent C_d-C_e bond, which leads to the formation of the d,e-$C_{70}O$ oxide (structure 5). The alternative process, where oxygen atom bridges the parent C_e-C_e bond (structure 4), was not observed. Interestingly, according to our previous calculations[14] which were performed on a set of empty fullerene oxides, the e,e-$C_{70}O$ should be the most stable isomer. Moreover, d,e-$C_{70}O$ was predicted to adopt the open oxidoannulene structure, where oxide formation leads to cleavage of the underlying C-C bond. Contrary to that, Li@d,e-$C_{70}O$ adopts a closed epoxide structure. As previously shown,[14] the preferred chemical structure of the C_{70} oxide (epoxide vs. oxidoannulene) depends on the actual electronic structure of the molecule. The only minima on the potential energy surfaces of a,b-$C_{70}O$ and c,c-$C_{70}O$ oxides in a singlet ground state refer to epoxides, whereas on the surfaces calculated in the lowest triplet state there are minima related to the open oxidoannulenes.[14] It is therefore not that surprising that d,e-$C_{70}O$ doped with Li may adopt the epoxide motif, in contrast to the empty isomer.

As discussed earlier, guest-to-cage electron transfer in the fullerene doped with K or Li is believed to serve as an explanation for the difference in reactivity of Li@$C_{70}O_3$ and K@$C_{70}O_3$ compared to that observed for the empty ozonides. To confirm this point we performed MD simulations for ozonides doped with a single H atom, as well as empty ozonide anions. In the first case the guest atom is in the $^2S_{1/2}$ electronic state, in common with Li or K, but it does not affect the electron structure of the fullerene cage as no electron or spin transfer can take place. As expected, these complexes behave in a similar way to empty ozonides and it is only for H@e,e-$C_{70}O_3$ that the spontaneous ring opening process following the (1) → (2) mechanism is observed. Contrary to that, the e,e-$C_{70}O_3^-$ anion, where the extra unpaired electron is imposed on the molecule, follows the (1)→(3)→(5) mechanism as observed for Li@e,e-$C_{70}O_3$.

Figure 4 and Table S6 (Supplementary Materials) summarizes the relative stabilities of the ozonide isomer series doped by the various guest atoms. For those isomers which do not undergo the above-described chemical reaction, the enthalpy was calculated as an average over the 20 ps molecular dynamics trajectory obtained at 298K. The numbers are presented relative to the enthalpy of the X@a,b-$C_{70}O_3$ isomer, which is the most stable of the empty ozonides. For e,e-$C_{70}O_3$, e,e-$C_{70}O_3^-$, K@e,e-$C_{70}O_3$ and Li@e,e-$C_{70}O_3$ we collected trajectories long enough to compute the enthalpy of the molecules. We also provide the enthalpy of the product of the ozone ring opening reaction following mechanism (1)→(2), which is labeled as e,e' or d,d' (for Ca@$C_{70}O_3$).

As discussed in ref. 14, addition of O_3 to a double bond in C_{70} leads to the thermodynamically preferred isomers a,b-$C_{70}O_3$ and c,c-$C_{70}O_3$, which are both close in enthalpy. The six other remaining theoretically possible isomers are less stable, with e,e-$C_{70}O_3$ being some 25.7 kcal mol^{-1} higher in enthalpy. The relative enthalpy of the group of a,a-$C_{70}O_3$, b,c-$C_{70}O_3$, c,d-$C_{70}O_3$ and d,e-$C_{70}O_3$ isomers is in the range 12.6 – 16.7 kcal mol^{-1}.

As was observed for complexes with light noble gas atoms,[11] the presence of the nitrogen atom does not influence the relative stabilities of the isomer series. This is consistent with the lack of any charge or spin transfer between the endohedral atom and the carbon cage in C_{70} or ozonide derivative. However, an entirely different order of relative enthalpy stability is observed for the ozonide isomers doped with an $^1S_0$ closed shell calcium atom. Now it is the Ca@a,a-$C_{70}O_3$ isomer which becomes the most stable, while the enthalpies of Ca@a,b-$C_{70}O_3$ and Ca@c,c-$C_{70}O_3$ are much higher. A lowering of the relative enthalpy is also observed for Ca@b,c-$C_{70}O_3$ and Ca@c,d-$C_{70}O_3$. Ca@e,e-$C_{70}O_3$ remains the least stable isomer, however the gap between its enthalpy and that of the reference Ca@a,b-$C_{70}O_3$ decreases. The pattern is clear: for complexes encapsulating a Ca atom, the products involving functionalization of single bonds (C_a-C_a, C_b-C_c, C_c-C_d, C_d-C_d, C_d-C_e,) are more stable than those of double bonds (C_a-C_b, C_c-C_c). The fact that the ozone ring opening reaction is detected for Ca@d,d-$C_{70}O_3$ instead of Ca@e,e-$C_{70}O_3$(when the empty e,e-$C_{70}O_3$ is more prone to dissociation than d,d-$C_{70}O_3$) can be rationalized if we assume that the dopant modifies the energy barriers for processes on the fullerene surface, as it does for the relative stabilities of the doped isomer series.

A very different pattern of stability is observed for radical ozonide complexes formed by encapsulating Li or K. In these cases the most stable isomers are X@d,d-$C_{70}O_3$, whereas the least stable isomers are those where the O_3 unit is attached to the equatorial belt. A group of five isomers, X@a,a-$C_{70}O_3$, X@b,c-$C_{70}O_3$ X@c,d-$C_{70}O_3$ as well as X@a,b-$C_{70}O_3$ and X@c,c-$C_{70}O_3$, have relative enthalpies that are just a few kcal mol^{-1} higher than the most stable isomer.

This difference in the stability ordering for the isomers of Li/K@$C_{70}O_3$ compared to their empty parent structures is not so surprising, and arises due to the transfer in charge and spin from the guest to the carbon cage, as discussed in earlier paragraphs. Again, to support this point we calculated the relative stability of ozonide isomers doped with a single H atom and for empty ozonide anions. The order of H@$C_{70}O_3$ isomer stabilities is essentially the same as observed for the empty fullerene series, whereas results for the $C_{70}O_3^-$ radical anions is very similar to that observed for complexes encapsulating K or Li.

In all analyzed sets of ozonides for which we were able to calculate enthalpies, the X@e,e-$C_{70}O_3$ isomer is the least stable irrespective of the presence and identity of the guest. It indicates that factors other than the electronic structure of the carbon cage might be important for the resulting properties of the C_e-C_e bond. It has been suggested that the local spheroid curvature of the carbon cage may influence the properties and reactivity of the fullerene surface.[29-30] The fact that C_e-C_e bonds are located in the flatter equatorial region is believed to be related to their limited reactivity.[31]

Conclusions

Depending on the identity of the endohedral guest, charge and/or spin density transfer can take place in complexes formed by C_{70} with individual Li, K ($^2S_{1/2}$ electronic state), and Ca atoms ($^1S_0$). No charge or spin transfer is observed for H ($^2S_{1/2}$) and N ($^4S_{3/2}$) guests. In the former cases modifications in the electron structure of the carbon cage directly influence the chemical properties of the fullerene surface, which is reflected in the relative stabilities of the $C_{70}O_3$ isomers doped with these atoms. Ozonides doped with H or N atoms exhibit properties similar to empty ones.

C_a-C_b and C_c-C_c double bonds seem to respond in a similar way to changes in the electronic structure of the carbon cage, as X@a,b-$C_{70}O_3$ and X@c,c-$C_{70}O_3$ isomers, which are the products of addition to a double bond, represent similar behavior in

all analyzed sets of complexes. Single bonds C_a-C_a, C_b-C_c, C_c-C_d also exhibit similar chemical properties. Yet another pattern of behavior should be expected for C_d-C_d and C_d-C_e bonds. Depending on the electronic state of the fullerene cage, adducts formed with these bonds exhibit relative stabilities that are similar to the products of functionalization of C_a-C_a, C_b-C_c and C_c-C_d single bonds or C_a-C_b and C_c-C_c double bonds. Functionalization of C_e-C_e should lead to the least stable isomer irrespective of the presence and identity of the endohedral guest.

New spontaneous chemical processes were observed in simulations of fullerenes doped with metal atoms. An endohedral calcium atom induces the ozone ring opening reaction for isomer Ca@d,d-$C_{70}O_3$, which does not occur for its empty parent complex. In Li@e,e-$C_{70}O_3$ the decomposition of the ozone ring proceeds following a different mechanism to the one typically observed for the empty fullerenes, leading to Li@d,e-$C_{70}O$ oxide and O_2. Finally, the presence of a calcium atom in the cage of the e,e isomer of the ozonide makes this isomer stable at room temperature, as no reaction is observed in the course of MD run, again contrary to the behaviour of the empty complex.

Our calculations therefore confirm that the chemical properties of fullerene surfaces can be tuned by the presence of an endohedral metal guest due to electron and spin transfer between the guest and the carbon cage. The reactivity of the surface and the stability of the products of fullerene functionalization depend directly on the electronic properties of the atom used to form the endohedral complex. It therefore seems that a judicious choice of metalofullerene as a reactant, instead of an empty fullerene, might result in the synthesis of new types of fullerene derivatives or in new isomers of known products.

Acknowledgments

Andrzej Bil would like to thank the Ministry of Science and Higher Education, Republic of Poland, for supporting this work under the grant no. N N204 280738 and to the Scientific Exchange Programme between the New Member States of the EU and Switzerland for financial support. Some calculations were performed at Wroclaw Network and Supercomputing Center.

References

(1) Popov, A. A.; Yang, S.; Dunisch L. *Chem. Rev.* **2013**, 113, 5989.

(2) Chaur, M. N.; Melin, F.; Ortiz, A. L.; Echegoyen, L. *Angew.Chem.-Int. Ed.* **2009**, 48, 7514.
(3) Yamada, M.; Akasaka, T.; Nagase, S. *Acc. Chem. Res.* **2010**, 43, 92.
(4) Lu, X.; Akasaka, T.; Nagase, S. *Chem. Commun.* **2011**, 47, 5942.

(5) Maeda, Y.; Tsuchiya, T.; Lu, X.; Takano, Y.; Akasaka, T.; Nagase, S. *Nanoscale* **2011**, 3, 2421.

(6) Tellgmann, R.; Krawez, N.; Lin, S. H.; Hertel, I. V.; Campbell, E. E. B., *Nature* **1996**, 382, 407.
(7) Gromov, A.; Krätschmer, W.; Krawez, N.; Tellgmann, R.; Campbell, E. E. B. *Chem. Commun*. **1997**, 20, 2003
(8) Almeida Murphy, T.; Pawlik, Th.; Weidinger, A.;Höhne, M.; Alcala, R.; Spaeth, J.-M. *Phys. Rev. Lett*., **1996,** 77**,** 1075.
(9) Benjamin S. C. et.al *J.Phys.:Condens. Matter* 18, **2006**, S867
(10) Heymann, D.; Bachilo, S.M.; Weisman, R.B.; *J. Am. Chem. Soc.* **2002**, 124, 6317**.**

(11) Bil, A.; Morrison, C.; *J. Phys. Chem. A* **2012**, 116, 3413.

(12) Bil, A.; Latajka, Z.; Morrison, C.; *Chem. Phys.* **2014**, 428, 121.

(13) Bil, A.; Latajka, Z.; Hutter, J.; Morrison, C.; *Chem. Phys.* **2014**, 433, 22.

(14) Bil, A.; Latajka, Z.; Morrison, C.; *J. Phys. Chem. A* **2009**, 113, 9891.

(15) Becke, A. *Phys. Rev A* 1988, 38 , 3098.

(16) Lee, C.; Yang, W.; Parr, R. *Phys Rev B* 1988, 37, 785.

(17) Lippert, G; Hutter, J.; Parinello, M.; *Mol. Phys.* 1997, 92, 477.

(18) Vande Vondele, J.; Krack, M; Mohamed, F; Parrinello, M; Chassaing, T; Hutter, J*. Comp. Phys. Commun.* **2005**, 167,103.

(19) The CP2K developers group, http://cp2k.org/

(20) Cole, R.; Salvetti, D. *Theor. Chim. Acta* **1975**, 37, 329.

(21) Grimme, S. *J. Comput. Chem.* **2004**, 25, 1463.

(22) Grimme, S. *J. Comput. Chem.* **2006**, 27, 1788.

(23) Silvestrelli, P. L. *Chem. Phys. Lett.* **2009**, 475, 285.

(24) Grimme, S.; Antony, J.; Ehrlich, S.; Krieg, H. *J. Chem. Phys.* **2010**, 132, 154104.

(25) Osuna, S.; Swart, M.; Sola, M., *J.Phys. Chem A* **2011**, 115, 3491.

(26) Goedecker, S.; Teter, M; Hutter, J. *Phys. Rev. B* **1996**, 54, 1703.

(27) VandeVondele, J.; Hutter, J. *J. Chem. Phys.* **2007,** 127, 114105.

(28) Mulliken, R. S.; *The Journal of Chemical Physics* **1955**, 23, 1833.

(29) Hawkins, J. M.; Meyer, A. ***Science*** 1993, 260, 1918-1920.

(30) Hawkins, J. M.; Meyer, A.; Solow, M. A. *J Am. Chem. Soc.* **1993,** 115**,** 7499.

(31) Thilgen, C.; Herrmann, A.; Diederich, F. *Angen Chem Int. Ed. Engl.* **1997,** 36, 2268.

Figure 1 Carbon atom and ring environments in C_{70}

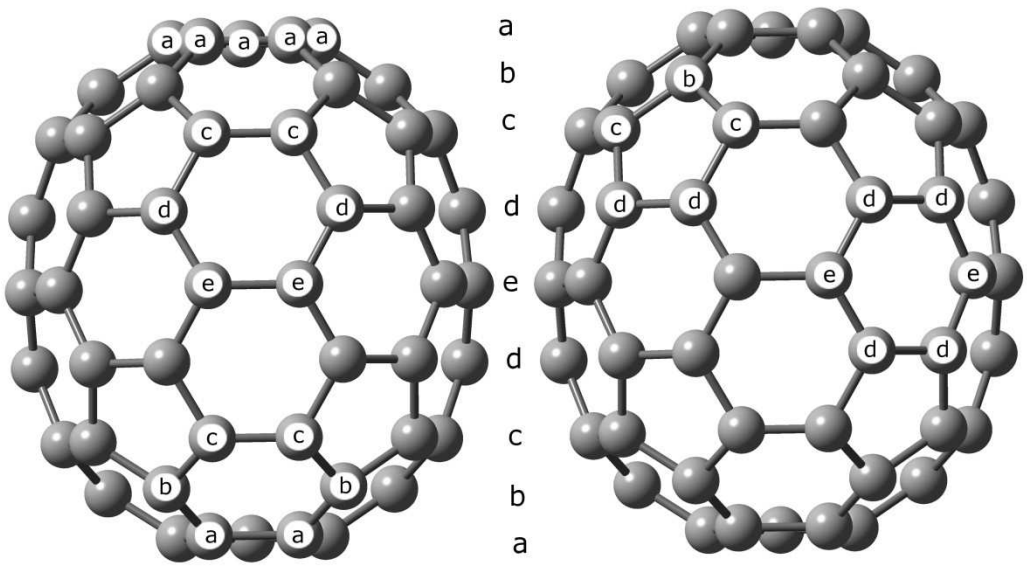

Figure 2 Schematic representation of the possible processes on the $C_{70}O_3$ surface**:** ozone ring opening (1→2), direct release of O_2 molecule (1→3), and two alternatives for oxide formation (3→4 over the parent C-C bond, or 3→5 over an adjacent C-C bond).

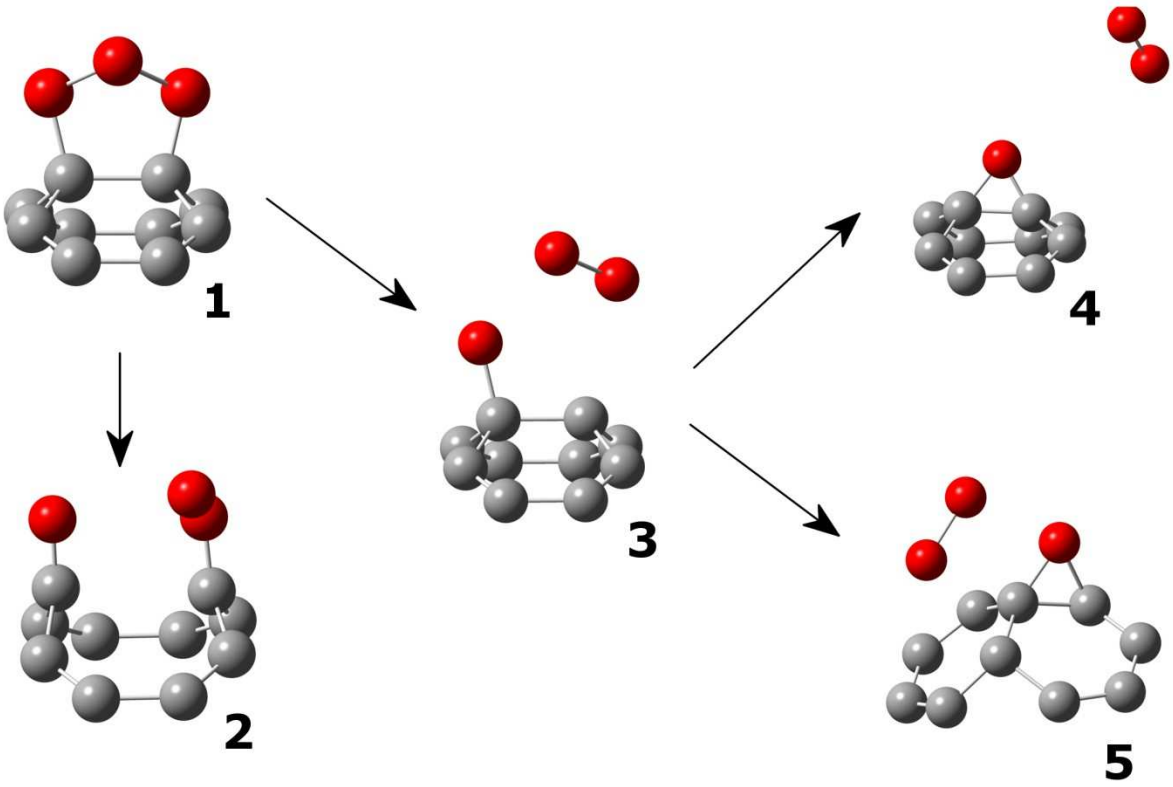

Figure 3 Trajectories arced by endohedral guest atoms inside a C_{70} cage during the course of MD simulations at 298K.

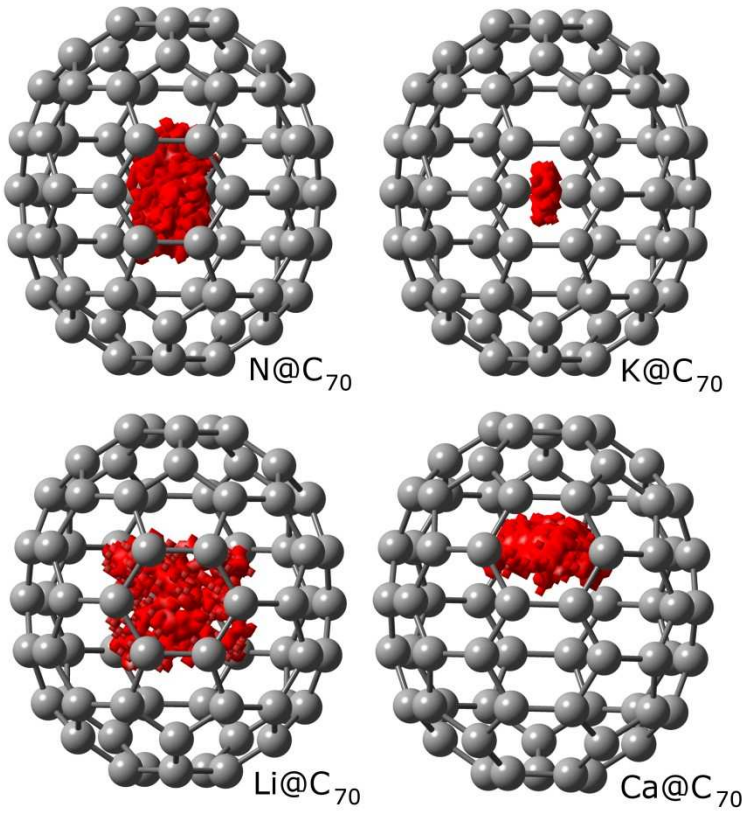

Figure 4 Enthalpies of $C_{70}O_3$, $C_{70}O_3^-$ radical anion, and X@$C_{70}O_3$ set of isomers, relative to the a,b-$C_{70}O_3$/X@a,b-$C_{70}O_3$ isomer. The guest atoms are H, Li and K ($^2S_{1/2}$ electronic state), N ($^4S_{3/2}$) and Ca ($^1S_0$). Note e,e' and d,d' denotes the product of the ozone ring opening reaction (process 1→2 on Figure 2) for e,e-$C_{70}O_3$, N@e,e-$C_{70}O_3$, H@e,e-$C_{70}O_3$, K@e,e-$C_{70}O_3$ and Ca@d,d-$C_{70}O_3$.

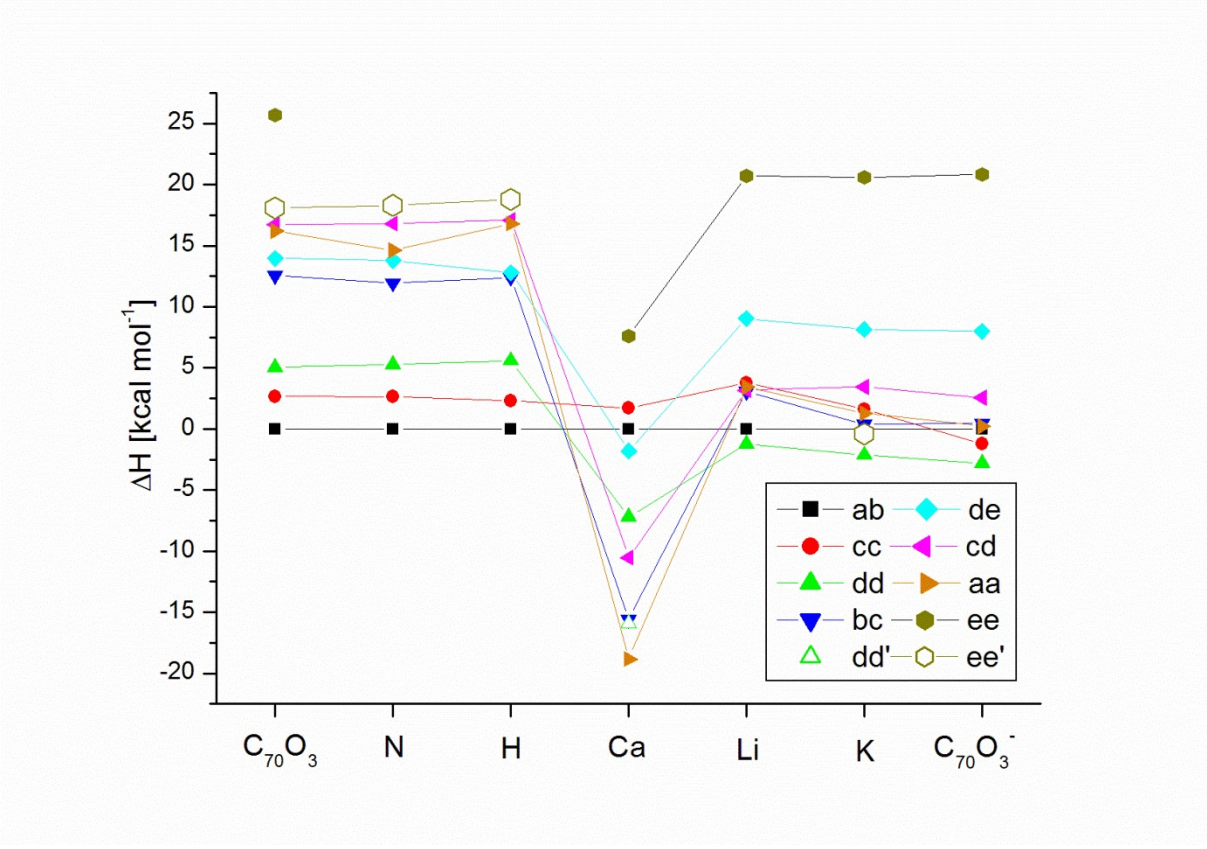

Graphical Abstract

A metal endohedral dopant modifies the relative stability of $C_{70}O_3$ ozonide isomer series.

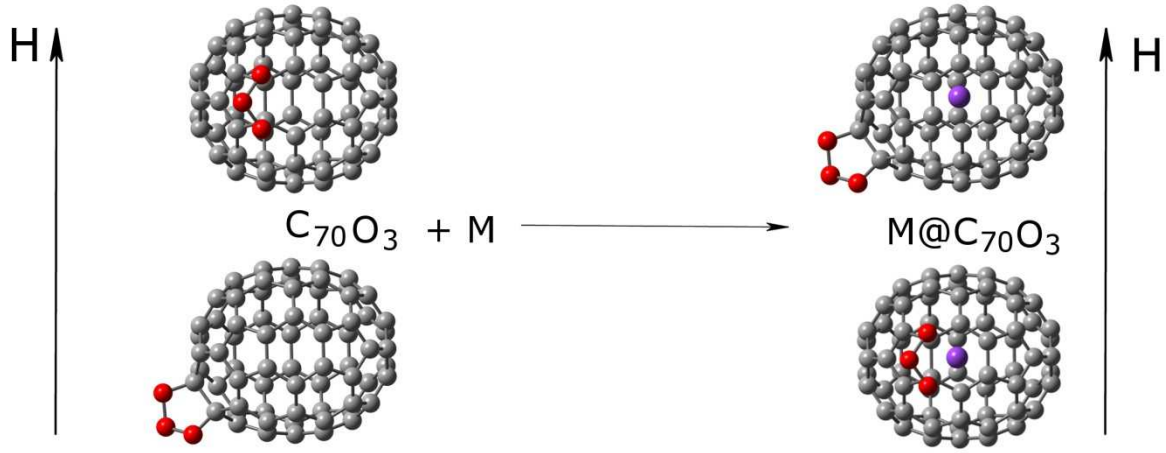

Electron transfer modifies chemical properties of C_{70} fullerene surface. An ab Initio molecular dynamics study of $C_{70}O_3$ molozonides doped with light atoms.

Andrzej Bil, Jürg Hutter, Carole A. Morrison

Supplementary Materials

Table S1 Time averaged atomic charges for X@C_{70}, where endohedral atom X= Ca, N, Li or K.

Atomic labelling is provided in Figure **S1** and in Table **S2**.

	Atomic charges					
	C_{70}	H@C_{70}	N@C_{70}	Ca@C_{70}	Li@C_{70}	K@C_{70}
C1	0.03	0.04	0.04	0.03	0.03	0.03
C2	0.00	0.00	0.00	-0.01	-0.01	0.00
C3	0.00	0.00	0.00	-0.01	0.01	-0.01
C4	0.04	0.04	0.04	0.02	0.03	0.03
C5	-0.01	-0.01	-0.01	-0.02	-0.01	-0.02
C6	-0.01	-0.01	-0.01	-0.02	-0.02	-0.01
C7	-0.08	-0.08	-0.08	-0.09	-0.08	-0.09
C8	-0.08	-0.08	-0.08	-0.09	-0.08	-0.08
C9	-0.01	-0.01	-0.01	0.00	-0.02	-0.02
C10	-0.01	-0.01	-0.01	0.00	-0.02	-0.02
C11	0.04	0.04	0.04	0.03	0.02	0.02
C12	0.00	0.01	0.00	-0.02	0.00	0.00
C13	0.00	0.00	0.00	-0.01	0.00	-0.01
C14	0.00	-0.01	0.00	-0.02	-0.01	-0.01
C15	0.04	0.04	0.04	0.02	0.03	0.03
C16	-0.01	-0.01	-0.02	-0.01	-0.02	-0.02
C17	-0.01	-0.02	-0.01	0.02	-0.01	-0.01
C18	-0.08	-0.07	-0.08	-0.11	-0.09	-0.09
C19	-0.08	-0.08	-0.08	-0.09	-0.08	-0.08
C20	0.14	0.13	0.15	0.11	0.13	0.11
C21	0.14	0.15	0.14	0.13	0.10	0.12
C22	-0.08	-0.08	-0.08	-0.08	-0.07	-0.08
C23	-0.08	-0.08	-0.08	-0.07	-0.08	-0.08
C24	0.15	0.14	0.14	0.11	0.12	0.12
C25	0.15	0.14	0.15	0.12	0.11	0.12
C26	-0.08	-0.08	-0.08	-0.10	-0.08	-0.08
C27	-0.08	-0.08	-0.08	-0.10	-0.07	-0.08
C28	-0.01	-0.02	-0.01	-0.02	-0.02	-0.01
C29	-0.01	-0.01	-0.01	-0.01	-0.02	-0.02
C30	0.04	0.04	0.04	0.03	0.03	0.03
C31	-0.01	-0.01	-0.01	0.00	-0.01	-0.01

C32	-0.01	-0.02	-0.01	-0.02	-0.02	-0.02
C33	-0.08	-0.08	-0.08	-0.08	-0.09	-0.07
C34	-0.08	-0.08	-0.08	-0.09	-0.08	-0.09
C35	0.15	0.15	0.14	0.11	0.08	0.12
C36	0.15	0.14	0.15	0.12	0.15	0.12
C37	-0.08	-0.08	-0.08	-0.08	-0.10	-0.08
C38	-0.08	-0.08	-0.08	-0.06	-0.08	-0.08
C39	-0.01	-0.02	-0.01	-0.02	-0.01	-0.02
C40	-0.01	-0.01	-0.01	-0.01	-0.02	-0.02
C41	0.04	0.04	0.04	0.03	0.03	0.03
C42	-0.01	-0.01	-0.01	-0.02	-0.01	-0.01
C43	-0.01	-0.01	-0.01	-0.01	-0.02	-0.02
C44	-0.08	-0.08	-0.08	-0.08	-0.08	-0.08
C45	-0.08	-0.08	-0.08	-0.06	-0.08	-0.08
C46	0.14	0.14	0.15	0.12	0.11	0.11
C47	0.14	0.15	0.15	0.11	0.10	0.11
C48	-0.08	-0.08	-0.08	-0.08	-0.07	-0.08
C49	-0.08	-0.08	-0.08	-0.10	-0.10	-0.08
C50	0.15	0.14	0.15	0.13	0.11	0.12
C51	0.15	0.14	0.14	0.11	0.11	0.11
C52	-0.08	-0.08	-0.08	-0.06	-0.08	-0.07
C53	-0.08	-0.08	-0.08	-0.07	-0.06	-0.09
C54	-0.01	-0.01	-0.01	-0.02	-0.03	-0.02
C55	-0.01	-0.01	-0.01	-0.01	0.00	-0.02
C56	0.04	0.04	0.04	0.02	0.03	0.03
C57	0.00	0.00	0.00	0.00	0.00	-0.01
C58	0.00	0.00	0.00	0.00	-0.01	-0.01
C59	0.00	0.00	0.00	-0.01	0.00	-0.01
C60	0.04	0.03	0.04	0.03	0.03	0.03
C61	-0.01	-0.01	-0.01	-0.02	-0.01	-0.01
C62	-0.01	-0.02	-0.01	-0.01	-0.02	-0.02
C63	-0.08	-0.08	-0.08	-0.07	-0.06	-0.08
C64	-0.08	-0.08	-0.08	-0.08	-0.08	-0.08
C65	-0.01	-0.01	-0.01	0.00	-0.01	-0.01
C66	-0.01	-0.02	-0.01	-0.03	-0.02	-0.02
C67	0.04	0.04	0.04	0.03	0.03	0.03
C68	0.00	-0.01	0.00	-0.01	-0.01	-0.01
C69	0.00	0.00	0.00	0.01	0.00	0.00
C70	0.04	0.04	0.04	0.02	0.03	0.03
endo	-	0.05	-0.05	0.53	0.51	0.57

Figure S1 Atoms labelling in C_{70}.

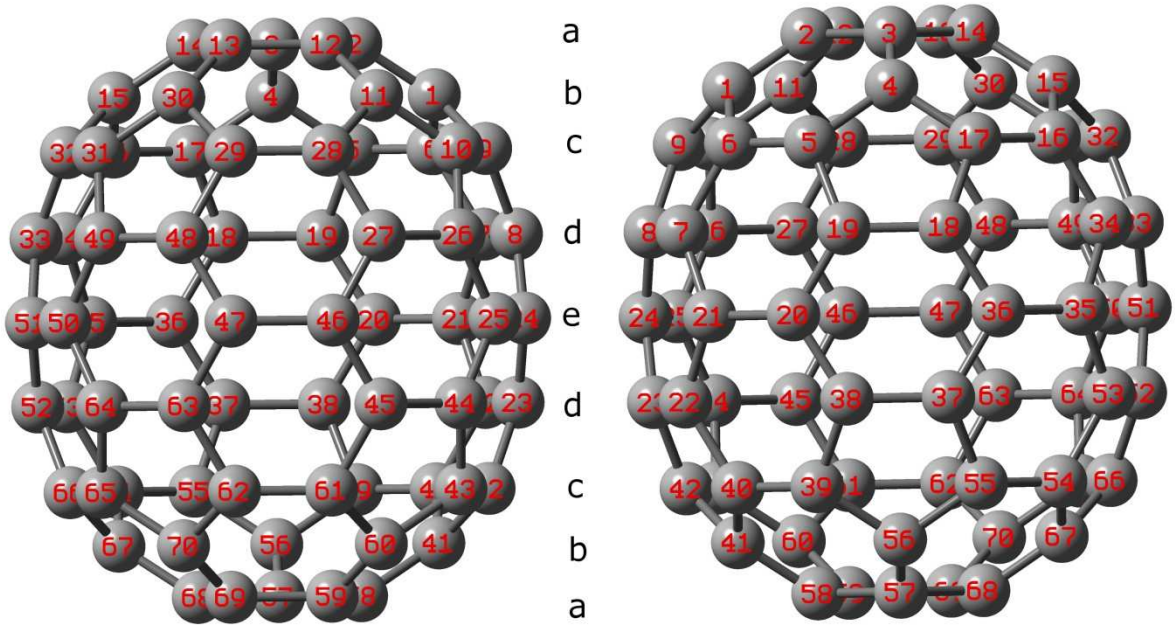

Table S2 Labels of atoms in C_{70} sorted by atomic layers.

layer	Atoms labels
a	2, 3, 12, 13, 14
b	1, 4, 11, 15, 30
c	5, 6, 9, 10, 16, 17, 28, 29, 31, 32
d	7, 8, 18, 19, 26, 27, 33, 34, 48, 49
e	20, 21, 24, 25, 35, 36, 46, 47, 50, 51
d	22, 23, 37, 38, 44, 45, 52, 53, 63, 64
c	39, 40, 42, 43, 54, 55, 61, 62, 65, 66
b	41, 56, 60, 67, 70
a	57, 58, 59, 68, 69

Figure S2 Actual charges of the guest atoms in Ca/Li/K@C_{70} plotted against simulation time.

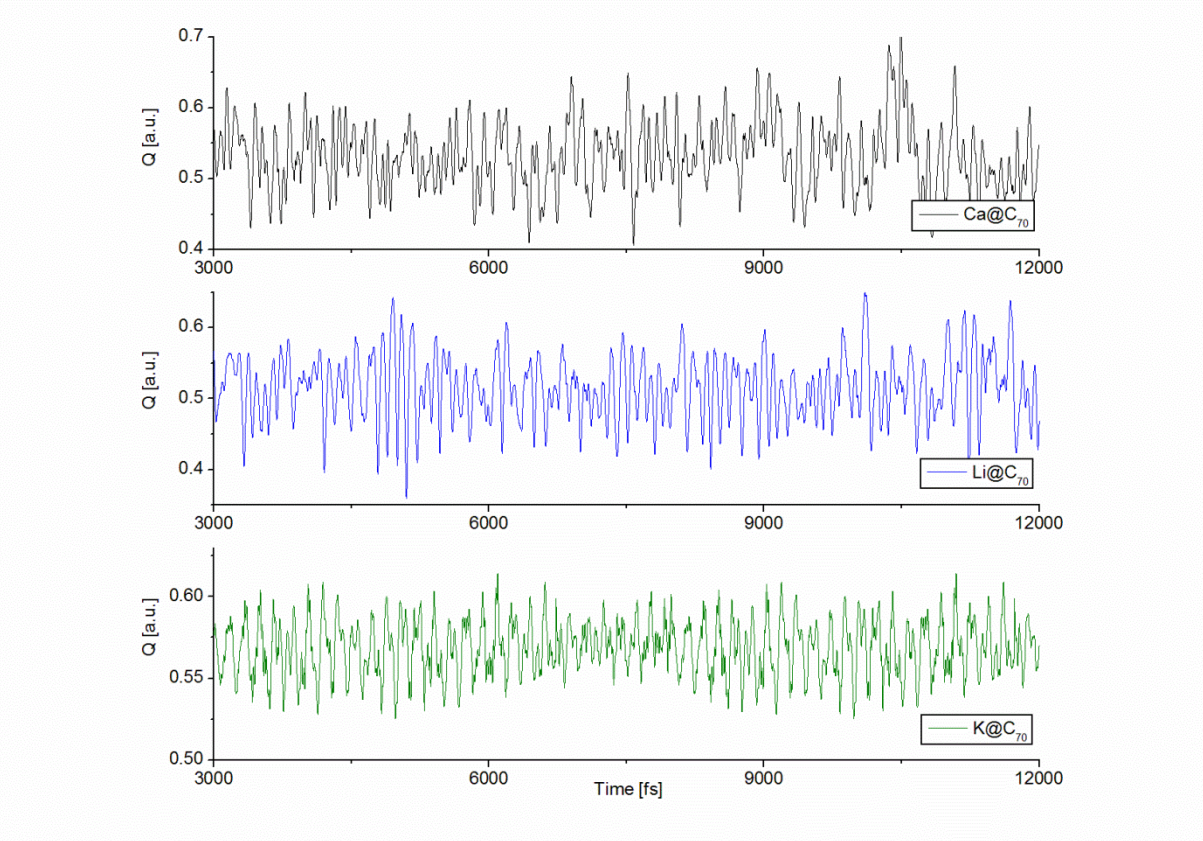

Table S3 Proportion of time [%] spent by the guest in the proximity of a center of the nearest carbon atom ring during the course of molecular dynamics runs at 298 K (see Figure 1 in the main text for ring labelling).

	C5, C6 ring				
	a-a-a-a-a	a-a-b-c-c-b	c-c-d-e-e-d	d-d-e-d-d-e	b-c-d-d-c
H@C_{70}	4.5	60.9	19.9	3.5	11.2
N@C_{70}	2.2	43.5	32.9	16.3	5.1
Li@C_{70}	0	5.0	45.3	26.4	23.3
K@C_{70}	0	0.3	65.7	33.9	0.1
Ca@C_{70}	0.3	55.7	27.8	1.0	15.2

Table S4 Average distance [Å] from the guest atom to the center of the nearest carbon atom ring in the course of molecular dynamics runs at 298 K (see Figure 1 in the main text for ring labelling).

	C5, C6 ring				
	a-a-a-a-a	a-a-b-c-c-b	c-c-d-e-e-d	d-d-e-d-d-e	b-c-d-d-c
H@C_{70}	2.47±0.14	2.47±0.14	2.46±0.16	2.46±0.18	2.48±0.12
N@C_{70}	2.74±0.08	2.73±0.18	2.90±0.21	2.96±0.20	2.67±0.15
Li@C_{70}	-	1.88±0.12	1.92±0.14	1.95±0.14	1.99±0.11
K@C_{70}	-	3.20±0.02	3.27±0.06	3.32±0.04	3.23±0.01
Ca@C_{70}	2.20±0.02	2.13±0.06	2.15±0.06	2.23±0.07	2.20±0.05

Figure S3 Trajectory of the endohedral K atom in K@C_{70} plotted against simulation time. The actual position of the atom inside the carbon cage is expressed by means of spherical coordinates. The radial distance R, azimuthal angle Θ and polar angle Φ are defined with reference to a local Cartesian coordinate system (see Figure **S4**) and satisfy the standard formulae: $R = (x^2 + y^2 + z^2)^{1/2}$; $\Phi = \arccos(z/R)$; $\Theta = \arctan(y/x)$. Note, the inverse tangent is defined so as to keep the azimuthal angle restricted to the interval $(-180^0, 180^0]$. Discontinuities observed when $\Theta(t) = 180^0$ are plotted as vertical jumps.

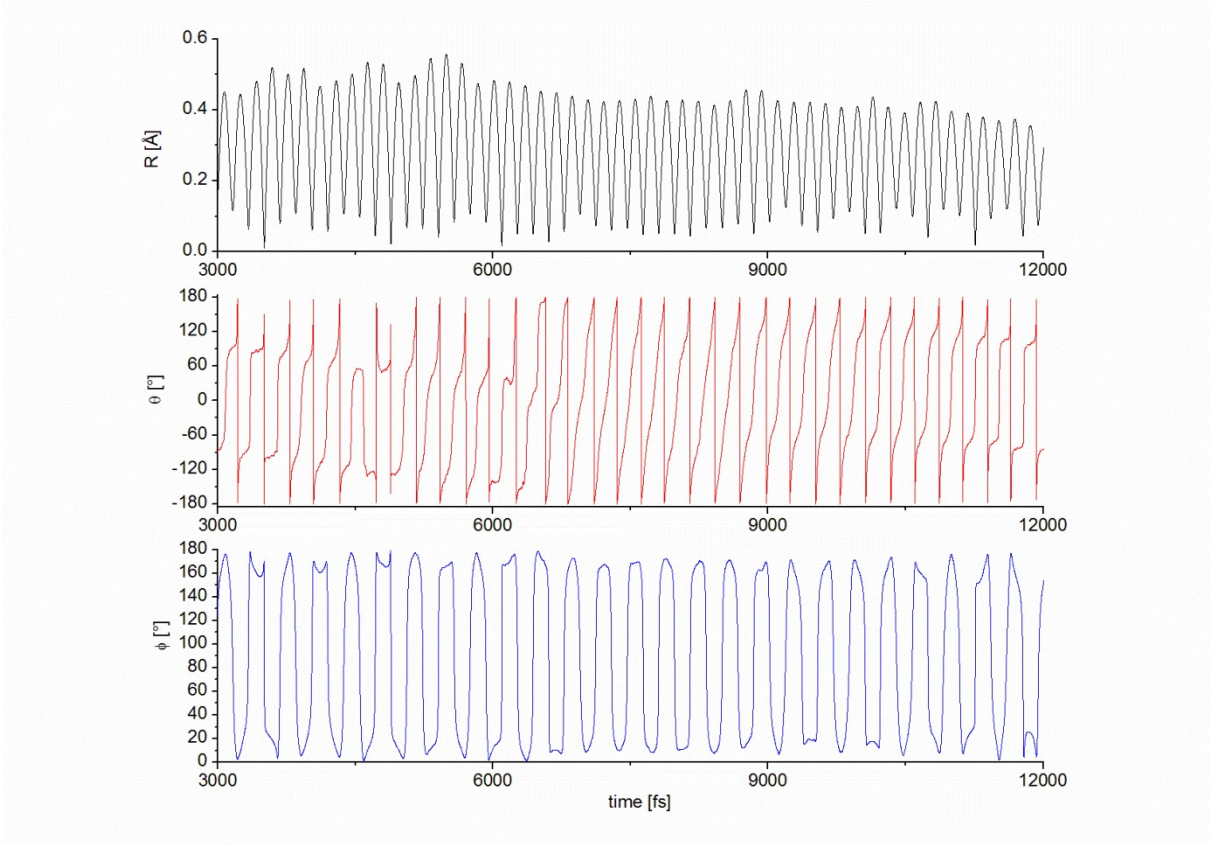

Figure S4 Cartesian coordinate system embedded in a C_{70} molecule (two projections). The origin (O) is defined by the center of mass of the fullerene molecule. OX axis points to the actual position of atom C21 in the equatorial belt; OZ axis, perpendicular to OX, points towards an a-type atom ring consisting of atoms 2, 3, 12, 13 and 14 (cf Figure S1 for atom labelling); OY axis is defined by a cross product of basis vectors of OZ and OX axes.

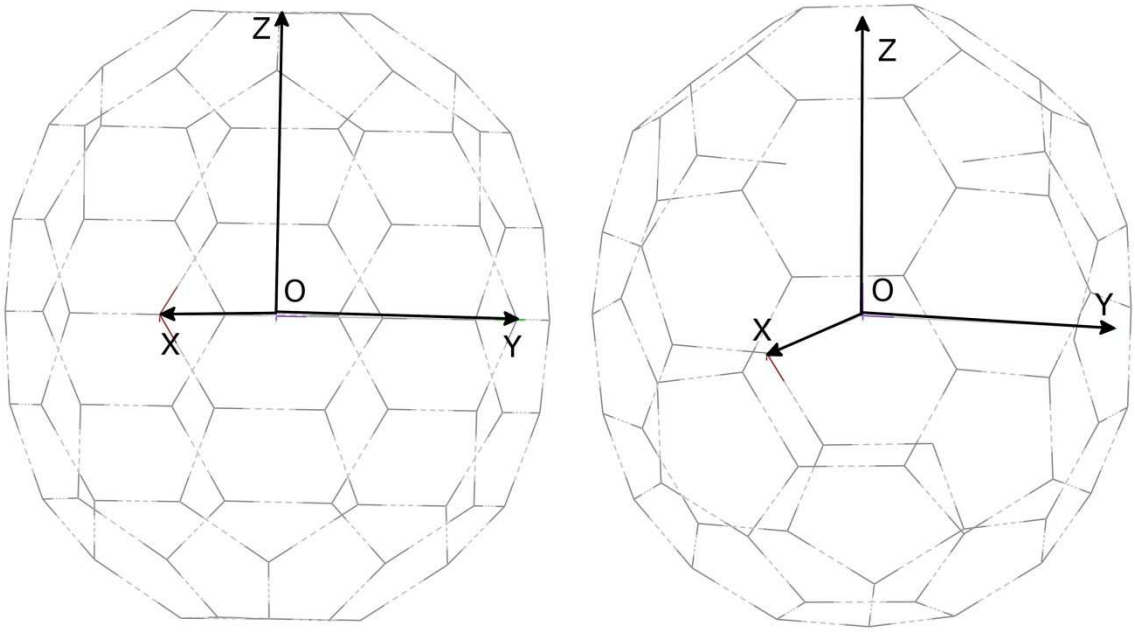

Figure S5 Trajectory of the endohedral N atom in N@C_{70} plotted against simulation time. The actual position of the atom inside the carbon cage is expressed by means of spherical coordinates.

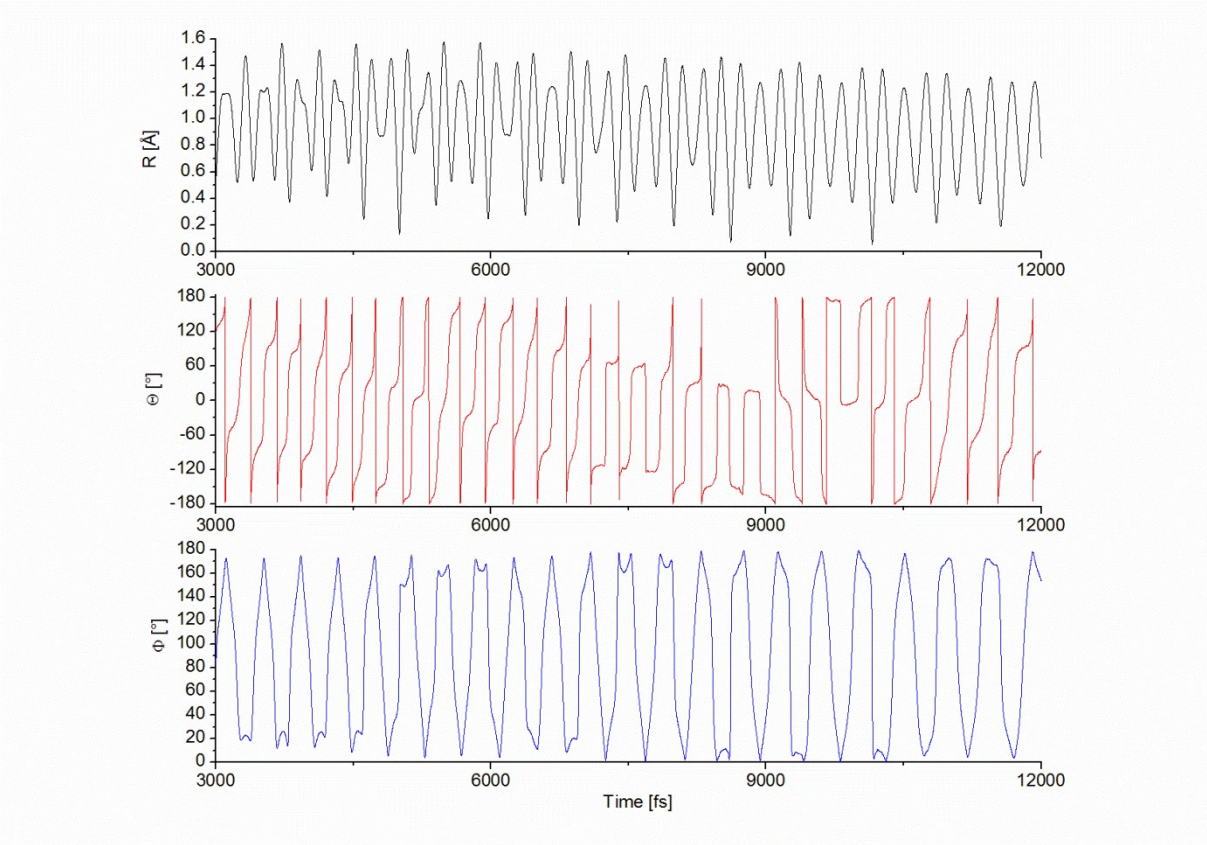

Figure S6 Trajectory of the endohedral Li atom in Li@C_{70} plotted against simulation time. The actual position of the atom inside the carbon cage is expressed by means of spherical coordinates.

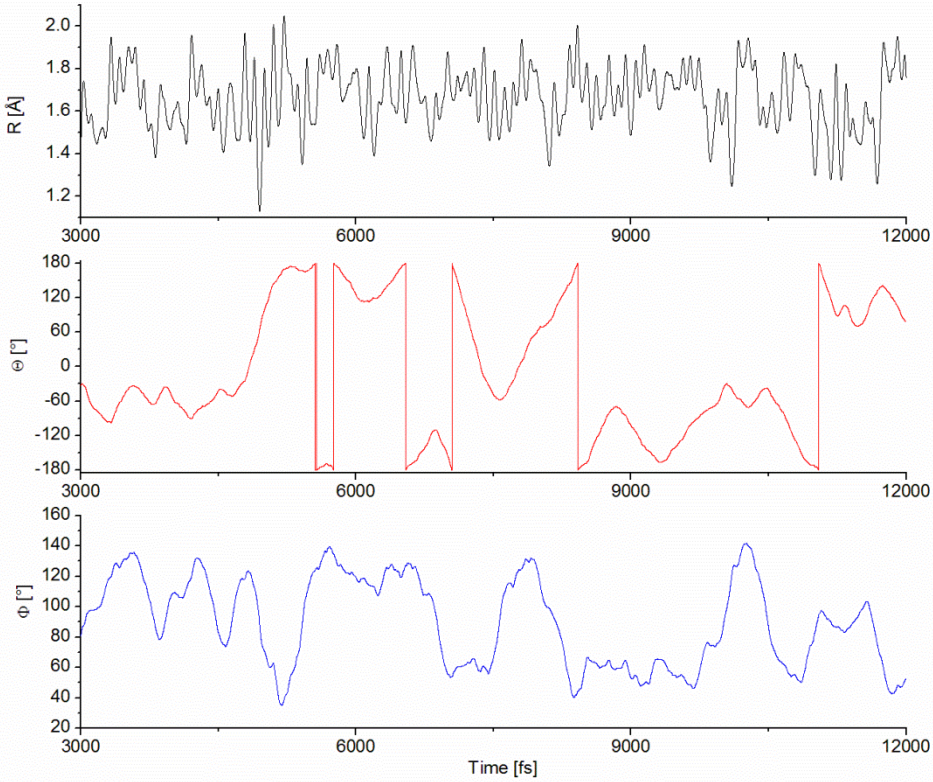

Figure S7 Trajectory of the endohedral Ca atom in Ca@C_{70} plotted against simulation time. The actual position of the atom inside the carbon cage is expressed by means of spherical coordinates.

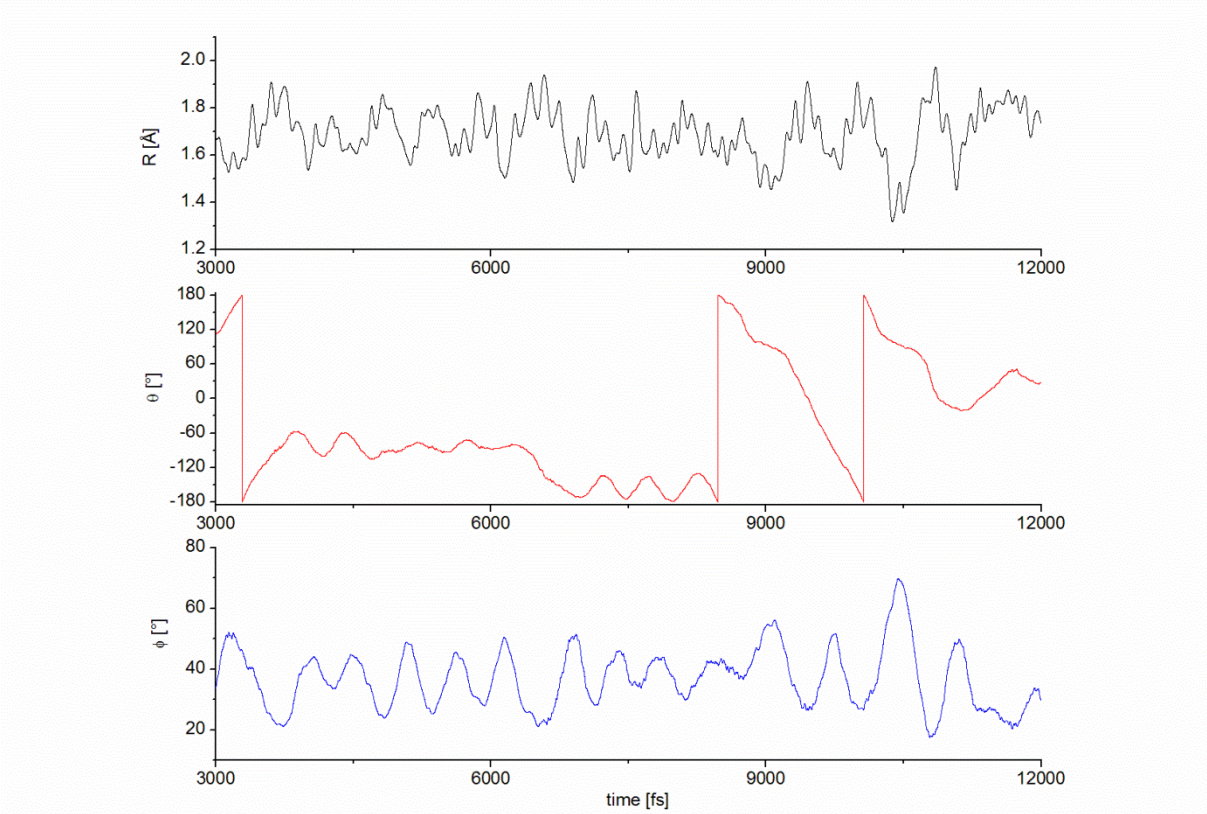

Figures S4-S7 indicate that the dynamics of the guest in X@C_{70} depends on the identity of the endohedral atom. The K atom undergoes small oscillations, keeping to the space around the fullerene gravity center. The N atom also oscillates, but it penetrates a much larger space and tends to be attracted by the inner surface of the cage. Li and Ca tend to undergo slow motions around the polar fullerene axis (as reflected in the plot of the azimuthal angle). The value of Φ, keeping to the range of 20-70^{o} for Ca@C_{70} indicates that this guest resides exclusively in only one hemisphere of the fullerene.

Table S5 Thermally averaged (298 K) volume [Å^3] of the carbon atom cage (calculated from the volume of the polyhedron established by the positions of the carbon nuclei) in C_{70} and X@C_{70}.

	Vol. (298K)
C_{70}	213.6±1.4
H@C_{70}	213.4±1.1

$N@C_{70}$	213.5±0.9
$Li@C_{70}$	214.6±1.0
$K@C_{70}$	215.2±1.1
$Ca@C_{70}$	215.2±1.1

Table S6
Average potential energies [kcal mol^{-1}] of the $C_{70}O_3$ and $X@C_{70}O_3$ set of isomers, relative to the *a,b*- isomer, obtained from MD trajectories (298 K).

	$C_{70}O_3$	$N@C_{70}O_3$	$H@C_{70}O_3$	$Ca@C_{70}O_3$	$Li@C_{70}O_3$	$K@C_{70}O_3$	$C_{70}O_3^-$
a,b	0	0	0	0	0	0	0
c,c	2.7	2.6	2.3	1.7	3.8	1.6	-1.2
a,a	16.2	14.6	16.8	-18.8	3.4	1.3	0.2
d,d	5.1	5.3	5.6	-7.2	-1.2	-2.1	-2.8
d,d'*	-	-	-	-15.9	-	-	-
b,c	12.6	11.9	12.4	-15.6	3.1	0.4	0.47
c,d	16.7	16.8	17.1	-10.5	3.2	3.4	2.6
d,e	14.0	13.8	12.8	-1.7	9.0	8.1	8.0
e,e	25.7	-	-	7.6	20.7	20.6	20.8
e,e'*	18.1	18.3	18.8	-	-	-0.4	-

* Product observed in the spontaneous ring-opening reaction recorded in the MD trajectory for $X@e,e\text{-}C_{70}O_3$ or $Ca@d,d\text{-}C_{70}O_3$